Journal of Photochemistry and Photobiology A: Chemistry 213 (2010) 7–13

Contents lists available at ScienceDirect

Journal of Photochemistry and Photobiology A: Chemistry

journal homepage: www.elsevier.com/locate/jphotochem

# Synthesis, third-order nonlinear absorption and refraction of fullerene dyads containing fluorene

Xinhua Ouyang[a,b], Gongchang Zeng[c], Heping Zeng[a,*], Wei Ji[b]

[a] Institute of Functional Molecules, School of Chemistry and Chemical Engineering, South China University of Technology, Guangzhou 510641, Guangdong, PR China
[b] Department of Physics, National University of Singapore, 2 Science Drive 3, Singapore 117542, Republic of Singapore
[c] Department of Chemistry, The University of Western Ontario, London, Ontario N6A 5B7, Canada

ARTICLE INFO

*Article history:*
Received 22 December 2009
Received in revised form 18 March 2010
Accepted 10 April 2010
Available online 21 April 2010

*Keywords:*
Fullerene–fluorene
Nonlinear optical properties
Two-photon absorption

ABSTRACT

Two new fullerene–fluorene dyads, *N*-methyl-2-(2-fluorenyl)-3,4-[60]fuller-pyrrolydine (**1**) and *N*-methyl-2-(2-fluorenyl)-3,4-[70]fullerpyrrolydine (**2**), were synthesized and their structures were confirmed by MALDI-MS, $^1$H NMR and FT-IR. Their electrochemical and optical properties were investigated by cyclic voltammetry and Z-scan technique, including, electronic potentials, two-photon absorption cross-sections ($\sigma_2$), nonlinear refractive indexes ($n_2$), microscopic second-order hyperpolarizabilities ($\gamma_R$) and third-order nonlinear susceptibilities ($\chi_I^{(3)}$ and $\chi_R^{(3)}$). Importantly, the $\chi_I^{(3)}$ and $\sigma_2$ in **2** were increased above 35% due to [70]fullerene unit than that of **1**.



## 1. Introduction

Functionalized fullerene derivatives have been studied extensively over the last decade owing to many particular features [1] and possible applications, ranging from medicine [2] to artificial photosynthesis [3], to material science [4]. Furthermore, particular attention has been devoted to their nonlinear optical (NLO) properties owing to their large π-conjugated surfaces and extensive charge delocalization [5]. A variety of donor–acceptor (D–A), donor–bridge–acceptor (D–π–A), donor–bridge–donor (D–π–D), multi-branched molecules, and organometallic molecules has been developed, and their structure–property relationships were investigated to develop organic materials with large third-order nonlinear absorption and refraction (TONA and TONF) [6]. The results of these studies reveal the TONA increases with the donor–acceptor strength, conjugation length and planarity of molecules.

Over the past decade, many fullerene dyads containing porphyrins [7], carbazole [8], tetrathiafulvalene [9], chlorines [10], amine [11] and ferrocenes [12] have been prepared and studied. However, there were still a very few publications about their third-order nonlinear absorption and refraction, especially fullerene derivatives at femtosecond timescale. Interestingly, with 9,9-dialkyl-diphenylaminofluorene (DPAF) as substitution [13], we obtained large two-photon absorptive cross-section, which was corresponding with the third-order NOL absorption. Meanwhile, it was also necessary to estimate the refractive index owing to its contribution to NOL refraction. Importantly, to our best knowledge, there was still no paper about refraction of fullerene dyads at femtosecond timescale. Therefore, fullerene based molecules are considered to be very promising candidates as photonic elements (e.g., optical switches and limiters) not only because of the inherent properties of fullerenes but also because fullerenes have been shown to enhance NOL performance, which also suggested us the possibility of investigating other dyads, such as fluorene. It was surprising that simple fullerene–fluorene dyads were not synthesized and studied. It was very significant to investigate the NOL properties between $C_{60}$/$C_{70}$ and fluorene, connecting them via the widely used pyrrolidine ring [14]. Actually, fluorene was extensively used as intermediate which may be acted as a spacer, or as an electron acceptor, or, eventually, as an energy transductor in fullerene dyads [15]. Moreover, fluorene can also be functionalized with a variety of substitutions and obtain excellent chemical and physical performance for the third-order NOL application.

We report here our results on two novel fluorene–fullerene dyads, *N*-methyl-2-(2-fluorenyl)-3,4-[60]fuller-pyrrolidine (**1**) and *N*-methyl-2-(2-fluorenyl)-3,4-[70]fuller-pyrrolidine (**2**), whose structures are shown in Scheme 1. The aim was to investigate how differently electronic acceptors influence their NOL properties by measuring the linear absorption spectra, open-aperture Z-scans, closed-aperture Z-scans and DFT calculations.

* Corresponding author. Tel.: +86 20 87112631; fax: +86 20 87112631.
*E-mail addresses:* hpzeng@scut.edu.cn, zenghp@scnu.edu.cn (H. Zeng).

1010-6030/$ – see front matter © 2010 Elsevier B.V. All rights reserved.
doi:10.1016/j.jphotochem.2010.04.008

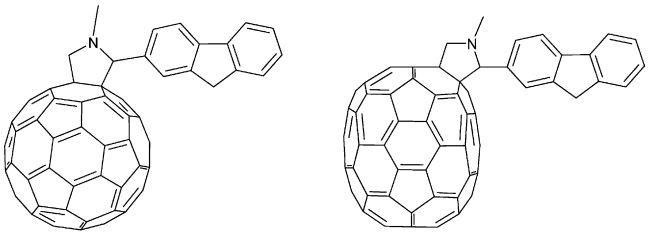

(1) (2)

**Scheme 1.** Structure of investigated fullerene dyads.

## 2. Experimental

### 2.1. Materials

*9H*-Fluorene-*2*-carbaldehyde, *N*-methylglycine, [60]fullerene and [70]fullerene were purchased from Tokyo Chemical Industry Co. Ltd. (TCI). All solvents were obtained from Guangzhou chemical reagent company in the experiments. The solvents were dried using standard procedures. All other reagents were used as received from commercial sources, unless otherwise stated.

### 2.2. Characterization

FT-IR spectra were recorded on a Perkin-Elmer Fourier transform infrared spectrometer and measured as KBr pellets. $^1$H NMR spectra were determined in $CDCl_3$ and $CS_2$ (3:1) with a Bruker DRX 400 MHz spectrometer. Chemical shifts ($\delta$) were given relative to tetramethylsilane (TMS). The coupling constants ($J$) were reported in Hz. Elemental analyses were recorded with a Perkin-Elmer 2400 analyzer. MALDI-TOF-MS spectra were acquired using a Voyager-DE STR MALDI-TOF mass spectrometer (PerSeptive Biosystems) in the linear positive mode with delayed extraction. Samples were analyzed using a dichloromethane solution of the sample (1 L) mixed with 10 L of dithranol matrix (10 mg mL$^{-1}$ in 70:30 $CH_2Cl_2$/EtOH) before loading onto a metal sample plate. Experiment course was monitored by TLC. Column chromatography was carried out on silica gel (100–200 mesh).

### 2.3. Synthesis of **1**

A mixture of $C_{60}$ (150 mg, 0.23 mmol), *9H*-fluorene-*2*-carbaldehyde (41 mg, 0.21 mmol), and *N*-methylglycine (82 mg, 0.92 mmol) was refluxed for 10 h in degassed anhydrous chlorobenzene under nitrogen atmosphere. After solvent removal, the residue was purified by chromatography with toluene and cyclohexane as eluent to give a black solid. Yield: 85.5 mg, 38.2%. FT-IR (KBr) $\nu$ (cm$^{-1}$): 3011.32, 2991.34, 1591.94, 1500.13, 1410.16, 1311.92, 1210.85, 1121.46, 1010.24, 831.22, 736.59, 713.24, 521.16; MALDI-TOF-MS ($M^+$): 940.5; $^1$H NMR ($CDCl_3 + CS_2$) $\delta$: 7.98 (s, 1H), 7.80 (d, 2H, $J$ = 5.6 Hz), 7.73 (d, 1H, $J$ = 7.6 Hz), 7.50 (d, 1H, $J$ = 7.6 Hz), 7.32 (t, 1H, $J$ = 7.6 Hz), 7.27–7.25 (m, 1H), 4.99 (s, 1H), 4.94 (d, 1H, $J$ = 4.8 Hz), 4.25 (d, 1H, $J$ = 8.2 Hz), 3.83 (s, 2H), 2.82 (s, 3H); elemental analysis: found: C 96.87, H 1.47, N 1.53, calculated for $C_{76}H_{15}N$: C 96.92, H 1.59, N 1.49.

### 2.4. Synthesis of **2**

A mixture of $C_{70}$ (201.1 mg, 0.24 mmol), *N*-methylglycine (76.1 mg, 0.86 mmol) and *9H*-fluorene-*2*-carbaldehyde (46.6 mg, 0.24 mmol) in dry chlorobenzene (230 mL) was heated at reflux under nitrogen for 8 h. After cooling the solution to room temperature, when the solvent was removed, the residue was purified by chromatography with toluene and cyclohexane as eluent to give a black solid. Yield: 48.1 mg, 18.9%. FT-IR (KBr) $\nu$ (cm$^{-1}$): 3017.19, 2987.28, 2911.37, 1601.21, 1498.46, 1407.55, 1319.09, 1116.64, 1008.73, 828.72, 793.86, 745.45, 671.12, 640.18, 471.94; MALDI-TOF-MS ($M^+$+1): 1060.8; $^1$H NMR ($CDCl_3 + CS_2$) $\delta$: 8.05 (d, 1H, $J$ = 7.6 Hz), 7.89 (d, 1H, $J$ = 8 Hz), 7.79 (d, 1H, $J$ = 7.8 Hz), 7.46 (t, 2H, $J$ = 7.8 Hz), 7.32–7.3 (m, 2H), 4.87 (s, 1H), 4.82 (d, 1H, $J$ = 4.8 Hz), 4.18 (d, 1H, $J$ = 8.2 Hz), 3.78 (s, 2H), 2.48, 2.58 (major isomer), 2.61 (s, 3H); elemental analysis: found: C 97.29, H 1.31, N 1.36, calculated for $C_{86}H_{15}N$: C 97.27, H 1.41, N 1.32.

### 2.5. Z-scans measurements

The nonlinear absorption and refraction were measured by a Z-scan technique. The laser pulses were produced by a mode-locked Ti:Sapphire laser (Quantronix, IMRA), which seeded a Ti:Sapphire regenerative amplifier and focused onto a 1-mm thick quartz cuvette containing the solutions of these molecules with the minimum beam waist of $21 \pm 1$ μm. The incident and transmitted laser pulse energy were monitored by moving the cuvette along the propagation direction of the laser pulses. The Z-scans confirmed that the samples had surprisingly good photo-stability, which was verified by indifference between the linear absorption spectra measured before and after intense laser irradiation in the Z-scans. In addition, the two-photon absorption coefficients, $\beta$, were extracted from best fitting the experimental data, and the cross-sections were then calculated from the definition $\sigma_2 = \beta\hbar\omega/N$, where $\hbar\omega$ is the photon energy and $N$ is the molecular concentration. The Z-scan experimental system was calibrated using a piece of cadmium sulfide (CdS) bulk crystal as a reference because it possesses large 2PA at the wavelength of 780 nm and has been well investigated in our laboratory [16].

### 2.6. Pump-probe measurement

The time-resolved transient absorption measurement (or degenerate pump-probe experiment) was carried out using 450 fs laser pulses at 1 kHz repetition rate with lower average power to minimize accumulative thermal effects. The laser pulses were produced by the same laser used in the Z-scans described above. To eliminate any coherent effects, the polarizations of the pump and the probe pulses were perpendicular to each other. The pump and probe beams were focused onto the solutions of these samples with a minimum beam waist of 30 μm. The probe pulse energy was a small fraction (less than a few percentage) of the pump pulse energy.

### 2.7. Computational methods

All of the calculations of the four molecules in this work have been performed on the Huge computer origin 2000 server center using the Gaussian 03 program package [17]. Geometric and electronic structures of ground and anion states were studied by B3LYP/6-31G(d). The theoretical energy gaps of these molecules have been estimated from the highest-occupied molecular orbital (HOMO) and lowest-unoccupied molecular orbital (LUMO) gaps and the lowest excited energies, respectively. The compositions of molecular orbits were analyzed using the GaussView 3.0 program.

## 3. Results and discussions

### 3.1. Single-photon absorption

Single-photon absorption spectra (UV–vis) of **1** and **2** were recorded in air-saturated toluene. Spectral feature of **1** arises from two optical bands centered at 280 and 431 nm as shown in Fig. 1,

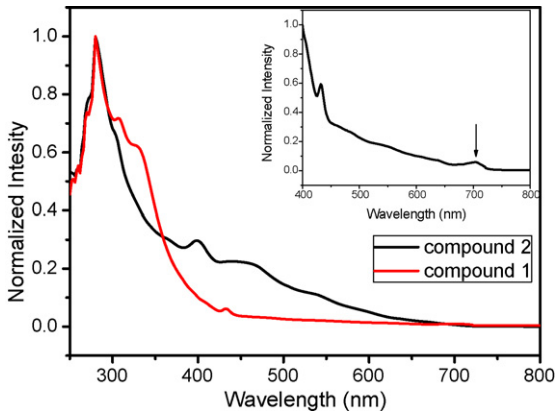


**Fig. 1.** UV-spectra of **1** and **2** and the absorption of **1** from 400 to 800 nm.

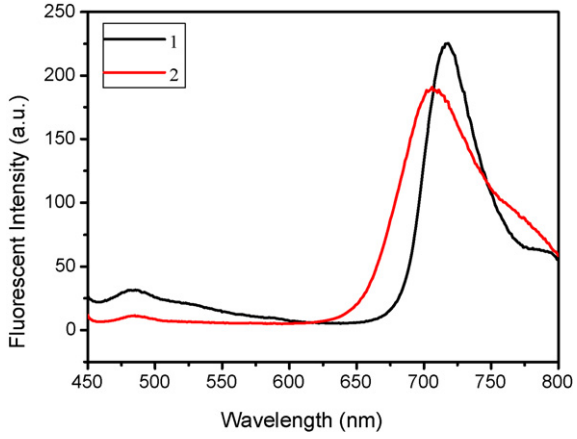


**Fig. 2.** The fluorescent spectra of **1** and **2**.

corresponding to the absorption of fluorene and $C_{60}$ cage moieties, respectively. As in Fig. 1 of **2**, the absorption is markedly stronger in visible region than that of **1**, the broad absorptive bands can be observed over a wide range in the visible region, with the main peak at 475 nm and 400 nm, which is similar with that of pristine $C_{70}$ due to low absorption of fluorene moiety in this region. The peak located at 280 nm is attributed to the absorption of fluorene moiety. Meanwhile, to differentiate the molecular contribution vs the number-sum component contribution to the measured UV–vis spectra, the absorption of two individual moieties was independently confirmed by the equivalent model *N*-methyl-[60]fulleropyrrolidine and fluorene, and optical bands appeared at 421 nm and 315 nm, respectively, which showed significant shift of the maximal peaks by comparison of **1**, it can be found that certain interactions exist between fluorene and $C_{60}/C_{70}$ moieties. Most importantly, an additional weak but characteristic long wavelength absorption band of the $C_{60}$ cage centered at roughly 705 nm was detected in the profile of **1** as shown in the insert of Fig. 1, giving the confirmation of **1** as $C_{60}$-conjugated structures with a similar ground to singlet excited-state energy gap.

### 3.2. Fluorescence properties of *1* and *2*

The fluorescence spectra of **1** and **2** in toluene are shown in Fig. 2 using 421 nm wavelength as excitation. The emissions of **1** and **2** were similar with that of fulleropyrrolidine [18], which was in agreement with the other experiments, pointing out the absence of any interaction between the two parts of the dyad in the ground state. Their maximal emissions of **1** and **2** are located at 717 and

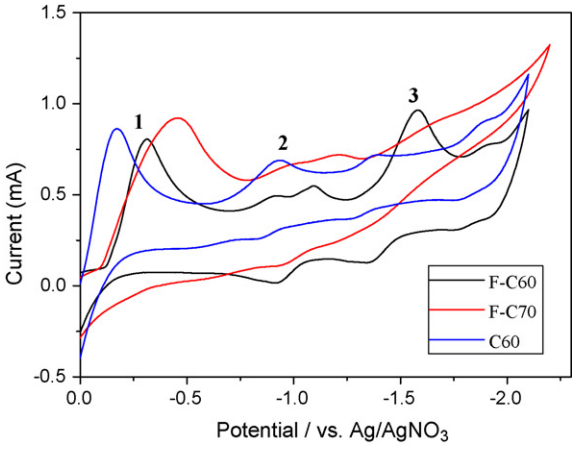


**Fig. 3.** Cyclic voltammograms of $C_{60}$, **1** and **2** at room temperature.

707 nm, a little shift was found between the two samples, it may be attributed to strength of the interaction in fullerene $C_{70}$ and $C_{60}$. Fluorescence measurements were also performed in benzonitrile, and benzene, giving analogous profile figures. That means that these dyads did not show solvent effects by different polar solvents.

### 3.3. Electrochemistry properties

The electrochemical behaviors of **1**, **2** and $C_{60}$, using benzyl cyanide as solvent at room temperature and $Bu_4NBF_4$ as the electrolyte, were characterized by cyclic voltammetry (CV). Fig. 3 shows the cyclic voltammograms in comparison with pristine fullerene ($C_{60}$). Although there were possible electronic interactions between the fullerene moieties, only three couples of reversible redox waves were observed in the accessible potential window of the solvent under the present conditions for **1** and **2**. The three well-defined redox waves (1, 2, and 3 in Fig. 3) observed for **1** and **2** shifted toward more negative potentials relative to pristine fullerene. This may be because of the predominantly inductive electronic interactions from the fluorene moiety, and/or the decrease of $\pi$-delocalization on the fullerene cage due to the introduction of two $sp^3$ carbon atoms. For **1** and **2**, the formal potentials of the first, second and three redoxes wave shifted cathodically comparing with the [60]fullerene, which strongly suggests the existence of electronic interplays between [60]fullerenes and fluorene moieties in the excited-states. Otherwise, comparing **1** with **2**, the first redox wave of **2** shifted cathodically, it can be seen that the interplays between [70]fullerene and fluorene moieties were stronger than that of **1**.

### 3.4. Two-photon absorption (2PA) properties of *1* and *2*

In the present study, the two-photon absorptive properties of **1** and **2** dissolved in $CS_2$ were investigated with femtosecond open-aperture Z-scans methods at 780 nm. The open-aperture Z-scan experimental system was calibrated using a piece of cadmium sulfide bulk crystal because this sample possesses large 2PA at the wavelength of 780 nm and was well investigated in our laboratory. The nonlinear optical properties of **1** and **2** are summarized in Table 1. Since the neat carbon disulfide showed large two-photon absorption in 780 nm, we also measured nonlinear absorption coefficient of carbon disulfide and give the value of 0.096 cm/GW, which was a similar range as the paper published recently [19]. Their open-aperture Z-scans results with concentration 0.001 M are plotted in Fig. 4 with three different incident intensities.

As shown in Fig. 4, **1** and **2** displayed positive signs for absorptive nonlinearities. According to the Z-scan theory for 2PA, we plotted

**Table 1**
Measured 2PA coefficients ($\beta$) and two-photon absorption cross-section values ($\sigma_2$) of compounds **1** and **2** ($\beta_{solution} = \beta_{solute} + \beta_{solvent}$).

| Compound/ solvent | [C] M | $\beta_{solution}$ (cm/GW) | $\beta_{solute}$ (cm/GW) | $\sigma_2$ ($\times 10^2$ GM) |
|---|---|---|---|---|
| $CS_2$ | | 0.096 | | |
| **1** | $1.0 \times 10^{-2}$ | 0.128 | 0.032 | 1.4 |
| | $1.0 \times 10^{-3}$ | 0.118 | 0.022 | 9.3 |
| | $1.0 \times 10^{-4}$ | 0.102 | 0.006 | 25.4 |
| **2** | $1.0 \times 10^{-2}$ | 0.138 | 0.042 | 1.8 |
| | $1.0 \times 10^{-3}$ | 0.126 | 0.03 | 12.7 |
| | $1.0 \times 10^{-4}$ | 0.106 | 0.01 | 42.4 |

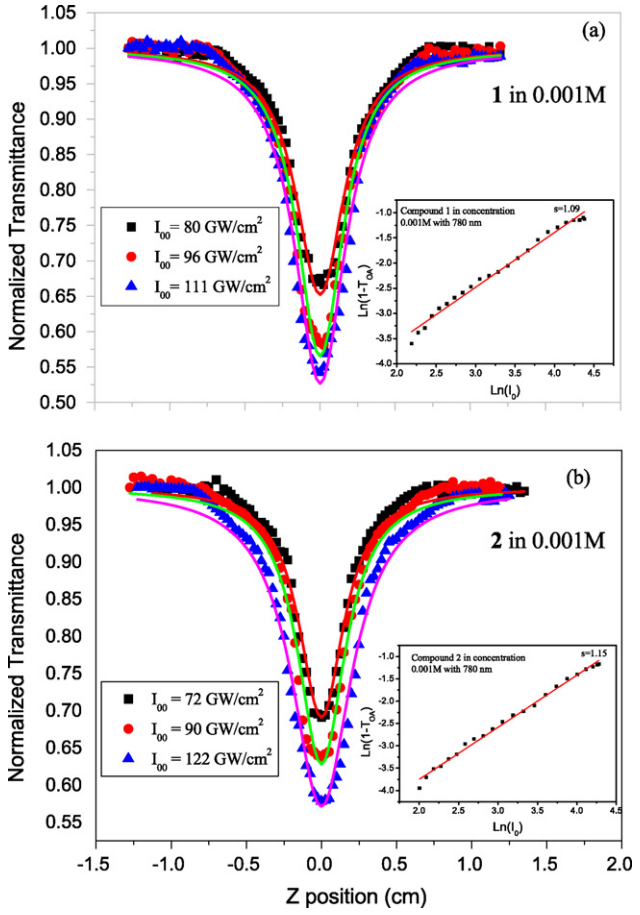


**Fig. 4.** Open-aperture Z-scans of **1** and **2** in CS2 with concentrations of 0.001 M.

the absorbance $(1 - T_{OA})$ (where $T_{OA}$ is the open-aperture transmittance) as a function of the maximum laser intensity on the *Z*-axis. The slopes of **1** and **2** were about one, which indicated the presence of 2PA in these dyads. The calculated values of 2PA coefficient ($\beta$) were 0.022 and 0.03 cm/GW for **1** and **2**, respectively, and the 2PA cross-sections ($\sigma_2$) were then derived as 930 and 1270 GM from $\sigma_2 = h\omega\beta/N$, where $N$ is the dyads densities. The imaginary part of the third-order nonlinear susceptibility of these dyads can be calculated through the relation $Im\ \chi^{(3)} = c^2 n_0^2 \beta\,(\mathrm{m/W})/240\pi^2\omega$, where $n_0$ is the linear refractive index, $c$ is the velocity of light in vacuum, and $\omega$ is the angular frequency of the light field. We calculate the values of $\chi_I^{(3)}$ for **1** and **2**, which are $9.16 \times 10^{-15}$ and $1.25 \times 10^{-14}$ esu, respectively. Then, we compared the 2PA cross-sections of these dyads and found that the $\sigma_2$ value and $\chi_I^{(3)}$ of **2** were improved about 35% by using [70]fullerene structure with the same substituent of **1**. We can conclude the strong electron-accepting group of $C_{70}$ can enhance significantly 2PA cross-section

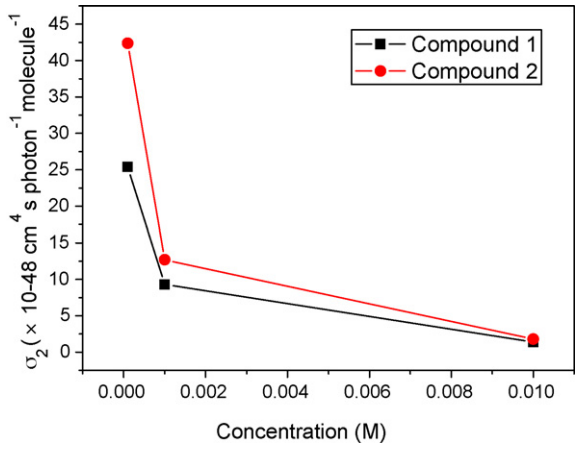


**Fig. 5.** Concentration dependence of 2PA cross-section values of **1** and **2**.

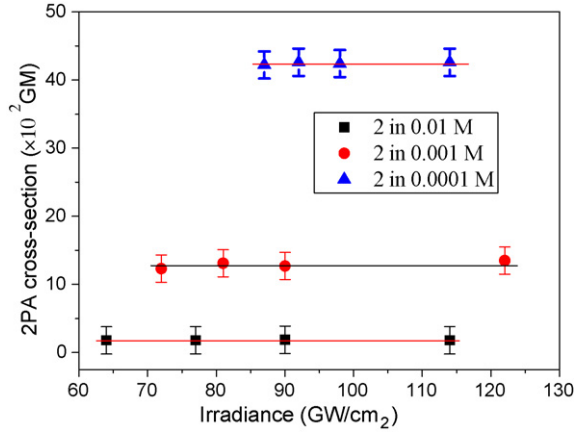


**Fig. 6.** Irradiance independence of 2PA cross-section values profile of **2**.

in the fullerene molecules system. Comparing the structure of **1** and **2**, we can find that the nonlinear responses are attributed form fullerene ($C_{60}$, $C_{70}$) unit. The determined roles of fluorene and the electron-accepting abilities of fullerene are calculated by Gaussian 03 software with B3LYP methods.

Consistent with the previous report [16] the 2PA cross-sections increase largely in a consistent trend, as the solution concentration is decreased from $10^{-2}$ to $10^{-4}$ M as shown in Table 1 and Fig. 5. Such concentration dependence has been attributed to molecule aggregation. Interestingly, with the high concentration ($10^{-2}$ M), the values of $\sigma_2$ are relatively close to each other in $1.4 \times 10^2$ and $1.8 \times 10^2$ GM, respectively, which indicate that the degree of molecule aggregation in the compounds **1** and **2** is almost the same due to the similar molecular structures. By decreasing the concentration to $10^{-3}$ M, the 2PA cross-sections ($\sigma_2$) increase to $9.3 \times 10^2$ and $12.7 \times 10^2$ GM, the values of **1** and **2** increase about seven times by comparing values of these dyads in concentration of 0.01 M. As the concentration decreases to $10^{-4}$ M, the degree of molecular separation increases at the low concentration. An increasing trend is observed form Fig. 5 and the 2PA cross-section increases to $25.4 \times 10^2$ and $42.4 \times 10^2$ GM for **1** and **2**.

As the scattering effects and exited-states absorption caused by high irradiance may influence the accuracy of overall 2PA cross-sections measured, we undertook the Z-scans of **1** and **2** in $CS_2$ with different irradiance. As an example, the results of **2** are shown in Fig. 6, and **1** also exhibited similar behaviors. We found that the measured $\sigma_2$ values apparently remain nearly constant in a straight line across the irradiance range from 64 to 122 GW cm$^{-2}$

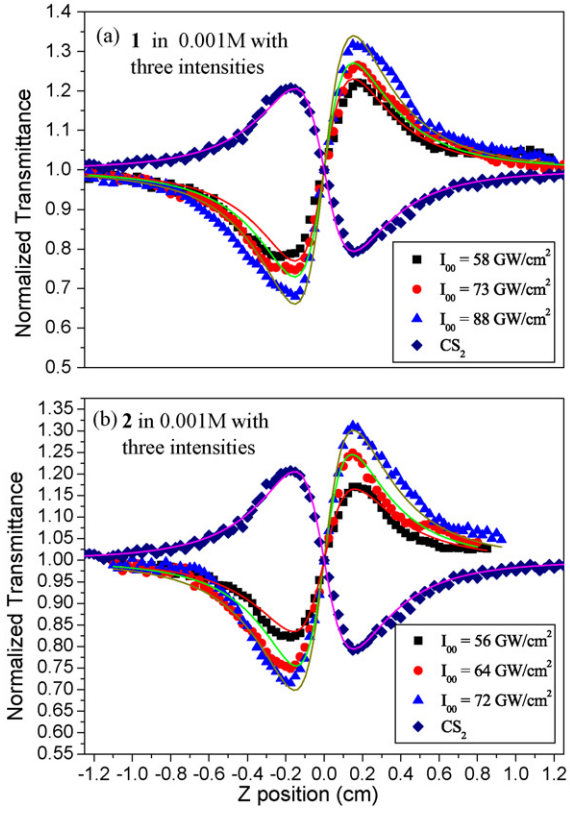


**Fig. 7.** The closed-aperture Z-scans of **1**, **2** and $CS_2$.

within the experimental errors with three different concentrations, confirming the independence of the laser intensity, which can be interpreted as the scattering and excited-state absorption, in particular singlet excited-state absorption, are negligible in our experiments.

### 3.5. Nonlinear refractive indexes of *1* and *2*

Closed-aperture Z-scan experiments of **1** and **2** confirm that they exhibited positive nonlinearity (Fig. 7) and solvent showed the negative signal. In the experiment, we find that the measured $n_2$ values of **1** and **2** were also independent of the irradiance by analyzing the results of closed-aperture Z-scans, which rules out the occurrence of higher-order refractive nonlinearities. Owing to the large nonlinear refractive index of $CS_2$, in order to extract the $n_2$ values of samples, we assumed a solution of noninteracting molecules. Moreover, the effective refractive nonlinearity in a pairwise additive model is given by $n_{2,\text{solution}} = (1-f)n_{2,\text{solvent}} + fn_{2,\text{solute}}$, where $f$ is the dilute solution containing a mole fraction of solute, and $n_{2,\text{solvent}}$ and $n_{2,\text{solute}}$ are the nonlinear refractive indices of solvent and solute, respectively. In our experiments, the value of $f$ is ~1.2%, and the $n_2$ is $-3.51 \times 10^{-7}$ cm$^2$/GW, in a similar range with the reported ones. The intrinsic nonlinear refractive indices, $n_{2,\text{solute}}$, obtained for **1** and **2** were $4.72 \times 10^{-5}$ and $4.8 \times 10^{-5}$ cm$^2$/GW, respectively. The real part of the third-order nonlinear susceptibility of these dyads can be calculated by the relation of $Re\ \chi^{(3)}\,(\text{esu}) = cn_0^2 n_{2,\text{solute}}\,(\text{m}^2/\text{W})/120\pi^2$, where $n_0$ is the linear refractive index, and $c$ is the velocity of light in vacuum. The measured values of $\chi_R^{(3)}$ for **1** and **2** were $3.17 \times 10^{-12}$ and $3.22 \times 10^{-12}$ esu, respectively. To estimate the contribution of one molecule to the third-order optical nonlinearity, it was convenient to define molecular nonlinear properties, which are termed molecular second-order hyperpolarizability $\gamma_R$. The $\gamma_R$ value is given by $\gamma_R = \chi_R^{(3)}/NL^4$, where $L$ is the

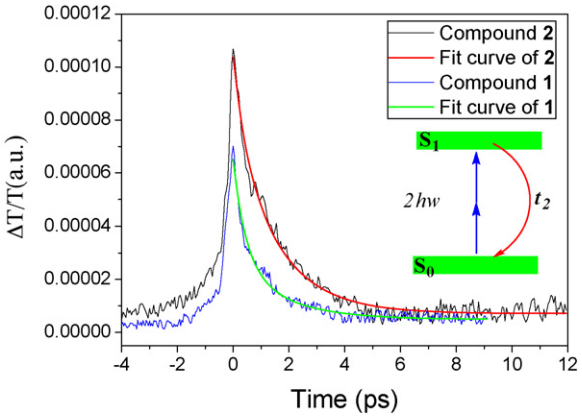


**Fig. 8.** Transient transmission measurements of **1** and **2**.

local field factor expressed by $L = (n_0^2 + 2)/3$, and $N$ is the density of molecules in the unit of number of molecules per cm$^3$. The calculated values of $\gamma_R$ at 780 nm for **1** and **2** were $9.1 \times 10^{-34}$ and $9.3 \times 10^{-34}$ esu, respectively. The $\gamma_R$ values were in the same order of magnitude as the measurement by Zhao et al. [20] for fullerene derivatives. By comparing the $\gamma_R$ of **1** and **2**, we can find clearly the values of $\gamma_R$ were very near owing to the similar structures of **1** and **2**.

### 3.6. Pump-probe properties of *1* and *2*

To study more details about the observed nonlinearities, we also conducted a degenerate pump-probe experiment with 450 fs, 780 nm laser pulses close to the 2PA peak positions of **1** and **2** in toluene solution. As shown in Fig. 8, the relaxation process may be described quantitatively by using a double-exponential fitting: $\Delta T/T = A_1 \exp(-t/\tau_1) + A_2 \exp(-t/\tau_2)$, where the fastest component, $\tau_1$, about 0.45 ps, is found to be independent of the pump intensity and is interpreted as the auto-correlation between the pump and probe pulses. The slowest component, $\tau_1$, on the picosecond scale is attributed to radiative, band-to-band recombination. The maximum transmittance change ($\Delta T/T$) in these solutions was found to be positive changes, showing reverse saturation absorption. In the meanwhile, we also found the magnitude of $\Delta T/T$ of these samples was consistent with the order of **2** > **1**, in agreement with that of the previously discussed Z-scans. Furthermore, the response time of these samples was evaluated to be 1.52 and 1.71 ps for **1** and **2**, respectively. In this time scale, it would be impossible for intramolecular energy transfer from the side group moiety to the fullerene moiety. Furthermore, it would be impossible for triplet excited-state absorption to occur since typical inter-system crossing times between singlet and triplet excited-states are a few nanoseconds. All these experiments assured that the measured $\sigma_2$ values result mainly from TPA processes.

### 3.7. Theoretic calculation of *1* and *2*

Owing to monofunctionalization of $C_{70}$ preferentially affords three kinds of isomers, C(1)–C(9) adduct (**2a**), with the (C7)–C(8) adduct (**2b**) being the second most favored, consequently, C(22)–C(23) adduct (**2c**), we used theoretical methods to investigate the relationships of these isomers. Meanwhile, their electron-accepting abilities were also predicated in **1** and **2** by adding an electron to these dyads during the optimization. Fig. 9 plots the optimized structures of **1** and **2** by DFT method with B3LYP/6-31G (d,p).

The optimized energies, methods, dipolar and point groups of **1** and **2** are summarized in Table 2. As shown in the table, all of three

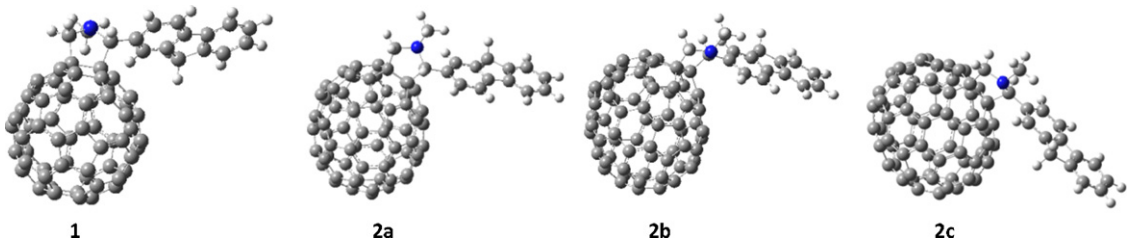


**Fig. 9.** The stereograph of optimized **1** and **2** by DFT//B3LYP/6-31G(d,p).

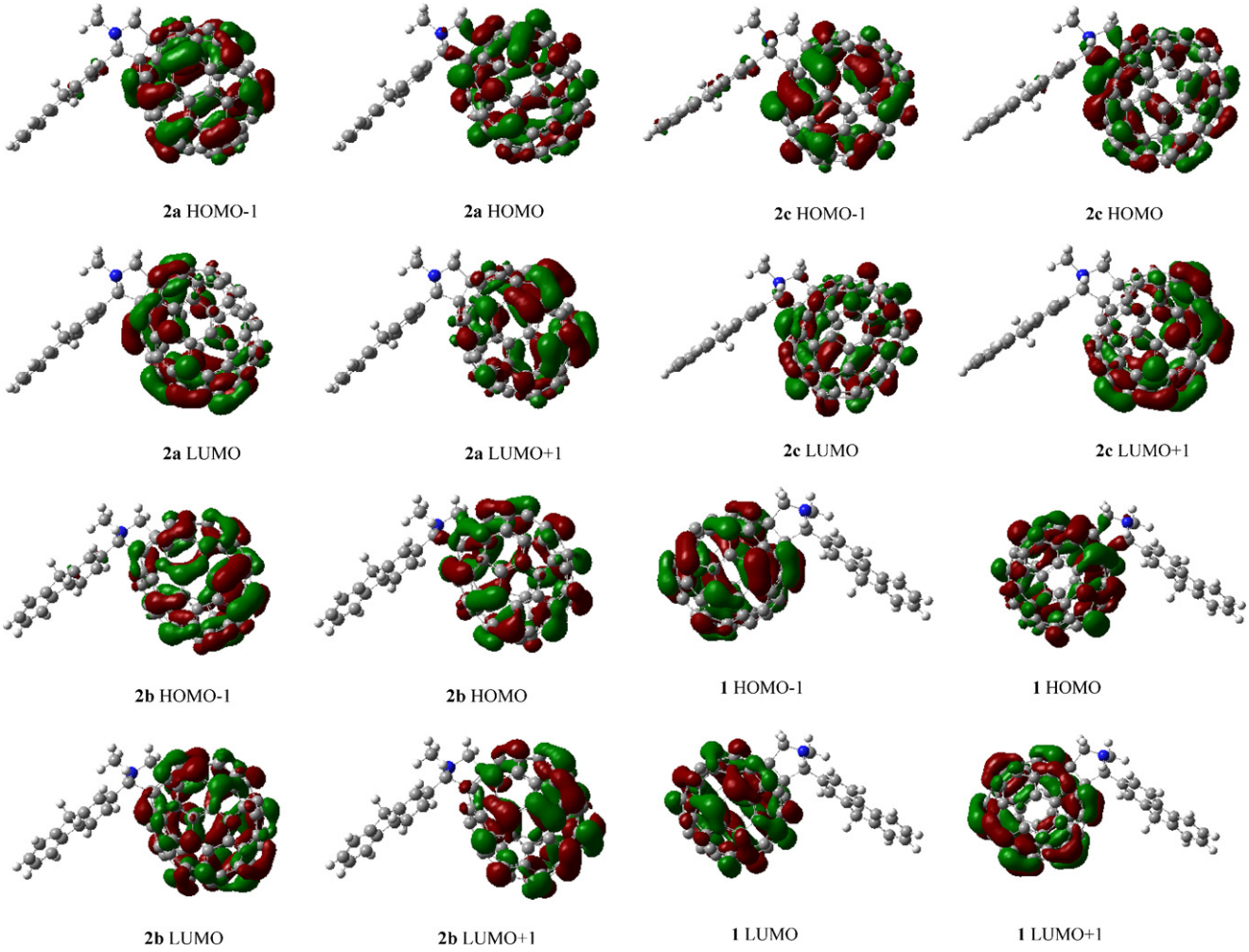


**Fig. 10.** The electronic densities of HOMO − 1, HOMO, LUMO and LUMO + 1 of **1** and **2**.

isomers' energies of **2** were lower than that of **1**, which can be found that electron-accepted (EA) ability of $C_{70}$ was stronger than that of $C_{60}$ with the same conditions. Then, the isomers' energies of **2a** and **2b** in Table 2 were almost the same, which proved the activities of bonds C(1)–C(9) and (C7)–C(8) in the $C_{70}$ surface were also similar when the $C_{70}$ reacted with other moieties. However, in **2c**, the energy was −90869.83 eV, which was about 0.8 eV higher than that of **2a** and **2b**, the reaction at bond C(22)–C(23) was worse than that

**Table 2**
The methods, energies, dipolar and point groups of compounds **1** and **2** in ground states and anion states.

| | Method | Energy (eV) | Dipolar (D) | Point group |
|---|---|---|---|---|
| **2a** in ground state | B3LYP/6-31G(d,p) | −90870.64 | 4.2686 | C1 |
| **2a** in anion state | B3LYP/6-31G(d,p) | −90872.65 | 8.4662 | C1 |
| **2b** in ground state | B3LYP/6-31G(d,p) | −90870.51 | 4.0149 | C1 |
| **2b** in anion state | B3LYP/6-31G(d,p) | −90872.52 | 9.1799 | C1 |
| **2c** in ground state | B3LYP/6-31G(d,p) | −90869.83 | 3.5424 | C1 |
| **2c** in anion state | B3LYP/6-31G(d,p) | −90872.03 | 7.485 | C1 |
| **1** in ground state | B3LYP/6-31G(d,p) | −80503.61 | 3.2438 | C1 |
| **1** in anion state | B3LYP/6-31G(d,p) | −80505.59 | 8.7343 | C1 |

of C(1)–C(9) and (C7)–C(8) in the $C_{70}$ surface, but it can still exist stably in the system. Furthermore, it also proved why there were three isomers in **2**. In order to investigate the EA properties of **1** and **2**, their anion states (AS) were optimized and results showed, all the energies of anion states were lower than that of ground states (GS). The energies of **1** and **2** in GS and AS were about 2.07 and 1.98 eV, respectively, displaying strong electron-accepting abilities with the order of **2** > **1**, which was in good agreement with the experimental results of CV.

As fluorene can act as a spacer, electron acceptor and an energy transductor, we plotted the electronic density distributions of HOMO, HOMO − 1, LUMO and LUMO + 1 of **1** and **2** in Fig. 10. Three isomers have almost the same HOMO and LUMO energies with HOMO–LUMO gaps in the range from 2.31 to 2.5 eV. Their electron densities of the LUMO and HOMO were almost the same and localizes in the fullerene sphere, which indicated there was no interaction between the fullerene and fluorene in ground states. Therefore, the fluorene only act as an energy transductor in **1** and **2**.

## 4. Conclusions

We synthesized two new fullerene–fluorene dyads, *N*-methyl-2-(2-fluorenyl)-3,4-[60]fuller-pyrrolydine (**1**) and *N*-methyl-2-(2-fluorenyl)-3,4-[70]fullerpyrrolydine (**2**) for the third-order nonlinear optical materials. Their nonlinear optical properties were investigated by Z-scan technique such as two-photon absorption cross-sections ($\sigma_2$), nonlinear refractive indexes ($n_2$), microscopic second-order hyperpolarizabilities ($\gamma_R$) and third-order nonlinear susceptibilities ($\chi_I^{(3)}$ and $\chi_R^{(3)}$). The concentration dependence of **1** and **2** were studied and it was found that the value of $\sigma_2$ increased with decreasing the concentration. Meanwhile, the $\chi_I^{(3)}$ and $\sigma_2$ in **2** increased above 35% due to using [70]fullerene structure than that of **1**. Electrochemical properties were also studied by cyclic voltammetry and showed interactions existing between fullerene and fluorene moiety in the excited-states. Furthermore, the EA abilities of $C_{70}$, $C_{60}$ and the functions of fluorene in **1** and **2** were also predicated by DFT methods with B3LYP, results showed that fluorene moiety acted as transductor in these dyads with the order of **2** > **1**.

## Acknowledgements

Financial support from the National Natural Science Foundation of China (nos. 20671036, 2007A010500008 and 2008B010800030) and the National University of Singapore is gratefully acknowledged. Ouyang X.H. would like to acknowledge the receipt of the Doctorate Foundation from South China University of Technology (SCUT), Guangzhou and the China Scholarship Council.

## References

[1] P.J. Benning, F. Stepniak, J.H. Weaver, Electron-diffraction and photoelectron-spectroscopy studies of fullerene and alkali-metal fulleride films, Phys. Rev. B 48 (1993) 9086–9096.
[2] Z. Xu, Z.Y. Suo, X.W. Wei, D.X. Zhu, Progress in research of fullerenes' biological activities, Prog. Biochem. Biophys. 25 (1998) 130–135.
[3] J. Baffreau, S. Leroy-Lhez, N. Van Anh, R.M. Williams, P. Hudhomme, Fullerene $C_{60}$-Perylene-3,4: 9,10-bis(dicarboximide) light-harvesting dyads: spacer-length and bay-substituent effects on intramolecular singlet and triplet energy transfer, Chem. Eur. J. 14 (2008) 4974–4992.
[4] A. Kumar, S.K. Menon, Fullerene–ferrocene dyad linked by rigid bilinkage: synthesis, photophysical properties and application as copper ion sensor, J. Phys. Org. Chem. 22 (2009) 661–669.
[5] D.M. Guldi, Fullerenes: three dimensional electron acceptor materials, Chem. Commun. 5 (2000) 321–327.
[6] G.S. He, L.S. Tan, Q. Zheng, P.N. Prasad, Multiphoton absorbing materials: molecular designs, characterizations, and applications, Chem. Rev. 108 (2008) 1245–1330 (Washington, DC).
[7] A.S.D. Sandanayaka, T. Murakami, T. Hasobe, Preparation and photophysical, photoelectrochemical properties of supramolecular porphyrin nanorods structurally controlled by encapsulated fullerene derivatives, J. Phys. Chem. C 113 (2009) 18369–18378.
[8] H.P. Zeng, T.T. Wang, A.S.D. Sandanayaka, Y. Araki, O. Ito, Photoinduced charge separation and charge recombination in [60]fullerene-ethylcarbazole and [60]fullerene-triphenylamines in polar solvents, J. Phys. Chem. A 109 (2005) 4713–4720.
[9] M. Sierra, M.A. Herranz, S. Zhang, L. Sanchez, N. Martin, L. Echegoyen, Self-assembly of $C_{60}$–π-extended tetrathiafulvalene (exTTF) dyads on gold surfaces, Langmuir 22 (2006) 10619–10624.
[10] A.D. Darwish, A.G. Avent, H.W. Kroto, R. Taylor, D.R.M. Walton, Novel base-catalysed formation of benzo[b]furano[60]- and -[70]fullerenes, J. Chem. Soc. Perkin Trans. 2.10 (1999) 1983–1988.
[11] C.M. Tollan, P.R. Birkett, N.S. Allen, The synthesis of high-content fullerene functionalised polymers through the controlled addition of an amine-tagged fullerene derivative, New J. Chem. 32 (2008) 1373–1378.
[12] E. Xenogiannopoulou, M. Medved, K. Iliopoulos, S. Couris, M.G. Papadopoulos, D. Bonifazi, C. Sooambar, A. Mateo-Alonso, M. Prato, Nonlinear optical properties of ferrocene– and porphyrin–[60]fullerene dyads, ChemPhysChem 8 (2007) 1056–1064.
[13] H.I. Elim, S.H. Jeon, S. Verma, W. Ji, L.S. Tan, A. Urbas, L.Y. Chiang, Nonlinear optical transmission properties of $C_{60}$ dyads consisting of a light-harvesting diphenylaminofluorene antenna, J. Phys. Chem. B 112 (2008) 9561–9564.
[14] D. Benne, E. Maccallini, P. Rudolf, C. Sooambar, M. Prato, X-ray photoemission spectroscopy study on the effects of functionalization in fulleropyrrolidine and pyrrolidine derivatives, Carbon 44 (2006) 2896–2903.
[15] L. Sánchez, N. Martin, E. González-Cantalapiedra, A.M. Echavarren, G.M. Aminur Rahman, D.M. Guldi, Molecular panels for energy transduction in C-60-based conjugates, Org. Lett. 8 (2006) 2451–2454.
[16] X.H. Ouyang, H.P. Zeng, W. Ji, Synthesis, Strong two-photon absorption, and optical limiting properties of novel C-70/C-60 derivatives containing various carbazole units, J. Phys. Chem. B 113 (2009) 14565–14573.
[17] M.J. Frisch, G.W. Trucks, H.B. Schlegel, G.E. Scuseria, M.A. Robb, J.R. Cheeseman, V.G. Zakrzewski, J.A. Montgomery, R.E. Stratmann, J.C. Burant, S. Dapprich, A.D. Daniels, K.N. Kudin, M.C. Strain, O. Farkas, J. Tomasi, V. Barone, M. Cossi, R. Cammi, B. Mennucci, C. Pomelli, C. Adamo, S. Clifford, J. Ochterski, G.A. Peterson, P.Y. Ayala, Q. Cui, K. Morokuma, D.K. Malik, A.D. Rabuk, K. Raghavachari, J.B. Foresman, J. Cioslowski, J.V. Ortiz, B.B. Stefanov, G. Liu, A. Liashenko, P. Piskorz, I. Komaromi, R. Gomperts, R.L. Martin, D.J. Fox, T. Keith, M.A. Al-Laham, C.Y. Peng, A. Nanayakkara, C. Gonzalez, M. Chalacombe, P.M.W. Gill, B.G. Johnson, W. Chen, M.W. Wong, J.L. Andres, M. Head-Gordon, E.S. Replogle, J.A. Pople, GAUSSIAN 2003, Gaussian, Inc., Pittsburgh, PA, 2003, pp. 239–335.
[18] L.Y. Chinag, P.A. Padmawar, T. Canteenwala, L.S. Tan, G.S. He, R. Kanna, R. Vaia, T.C. Lin, Q. Zheng, P.N. Prasad, Synthesis of C-60-diphenylaminofluorene dyad with large 2PA cross-sections and efficient intramolecular two-photon energy transfer, Chem. Commun. 17 (2002) 1854–1855.
[19] H.I. Elim, R. Anandakathir, R. Jakubiak, L.Y. Chiang, W. Ji, L.S. Tan, Large concentration-dependent nonlinear optical responses of starburst diphenylaminofluorenocarbonyl methano[60]fullerene pentads, J. Mater. Chem. 17 (2007) 1826–1838.
[20] Y.M. Zhao, Y. Shirai, A.D. Slepkov, L. Cheng, L.B. Alemany, T. Sasaki, F.A. Hegmann, J.M. Tour, Synthesis, spectroscopic and nonlinear optical properties of multiple [60]fullerene-oligo(p-phenylene ethynylene) hybrids, Chem. Eur. J. 11 (2005) 3643–3658.